

Chromium reduction via a semi-conducting hematite electrode: implications for microbial cycling of metals in natural soils

Chen, Michael A.^{1,2}, Mehta, Neha^{1,3}, and Kocar, Benjamin D.^{1,4,}*

1. Parsons Laboratory, MIT, Department of Civil and Environmental Engineering, 15 Vassar St., Cambridge, MA, 02139

2. University of Minnesota, Department of Earth and Environmental Sciences, 116 Church St. SE, Minneapolis, MN 55455

3. Institut de Minéralogie, de Physique des Matériaux, et de Cosmochimie, Sorbonne Universités, 75005 Paris, France

4. Exponent, Inc., 15375 SE 30th Place, Suite 250, Bellevue, WA 98007

Keywords:

Abstract: Semi-conducting Fe oxide minerals, such as hematite, are well known to influence the fate of contaminants and nutrients in many environmental settings and influence microbial growth under suboxic to anoxic conditions through a myriad of different processes. Recent studies of Fe oxide reduction by Fe(II) have demonstrated that reduction of Fe at one surface can

result in the release of Fe(II) different one. Termed Fe(II) catalyzed recrystallization, this phenomena is attributed to conduction of additional electrons through the mineral structure from the point of contact to another which occurs because of the minerals' semi-conductivity. While it is well understood that Fe(II) plays a central role in redox cycling of elements, the environmental implications of Fe(II) catalyzed recrystallization need to be further explored. Here, we provide evidence that the Fe mineral conductivity underpinning Fe(II) catalyzed recrystallization can couple the reduction of Cr, a priority metal contaminant, with an electron source that is cannot directly affect Cr. This is shown for both an abiotic electron source, a potentiostat, as well as the metal reducing bacteria *Shewanella Putrefaciens*. The implications of this work show that semi-conductive minerals may be links in subsurface electrical networks that physically distribute redox chemistry and suggests novel methods for remediating Cr contamination in groundwater.

1. **Introduction**

Hematite's natural abundance and thermodynamic properties make it a central player in the cycling of many different contaminants and nutrients, and therefore a continuing focus for biogeochemical research.¹⁻¹¹ Hematite play an important role in the abiotic cycling of U, where reduction of hematite by sulfidization will result in the long term precipitation of reduced U/Fe solids.¹² Dissimilatory metal reducing bacteria (DMRB) can also rely on hematite in aquifers and soils as a primary electron sink for their anoxic metabolism.^{9,13} Biotic reduction by metal reducing bacteria is one of the primary drivers of Fe reduction in natural soils. A variety of mechanisms allow microbes to access these solid electron sinks, which include the use of microbial nanowires, release of electron carriers, such as cytochrome-C, as well as direct contact with minerals by surface colonization.¹³⁻¹⁷ Metal reducing bacteria use these mechanisms to

access electron acceptors at ranges as large as 10 μm to 20 μm , as well as access nanopores that are too small for cells to enter.^{16,18} Dissimilatory metal reducing bacteria (DMRB) have also been observed to use these mechanisms with conductive electrodes held at a reducing potential, which has provided the basis for development of microbial fuel cells.^{19,20}

Typically, Fe oxides are considered the terminal electron acceptor in bacterial metal reduction. However, recent studies using isotopically labeled Fe(II) have demonstrated that the semi-conductivity of hematite (and other similar Fe oxides) results in a dynamic cycling of the atoms within the mineral.²¹⁻²³ Further investigation of this phenomena revealed that the labeled Fe(II) initially in solution would sorb to one surface of the mineral and then an unlabeled Fe(II) would be released on another surface, thus bringing the mineral closer to isotopic equilibrium over time.^{24,25} This phenomena, termed Fe(II) catalyzed recrystallization, is postulated to arise from conduction of the electron donated by Fe(II) from the initial point of sorption to another point on the mineral, which is a direct result of the mineral's semi-conductivity. The primary focus of these studies has been understanding the cycling of Fe in these systems, but the implications of cycling of other elements or the influence on bacterial metal reduction have not been ignored.²⁶ Fe(II) catalyzed recrystallization has shown to influence metal cycling: recrystallization of Fe solids in the presence of U boosted incorporation of U into the Fe solid over long times, while recrystallization of Mn doped Fe solids resulted in enhanced release of Mn over time.^{27,28} It also has been explored with DMRB, showing that the Fe(II) produced by bacterial metal reduction can drive recrystallization and transformation of Fe solids.²⁹ One area that has not been investigated thoroughly, however, is how the conductivity that underpins Fe(II)-catalyzed recrystallization could mean that Fe oxides can electrically link redox reactions. In this scenario, a redox reaction (such as bacterial metal reduction) may occur on one surface of

a semi-conductive Fe oxide, and the resulting electron may be delivered to another surface that can then drive redox reactions at that physically distinct surface. A recent study has explored this possibility with the model compound, cytochrome-c, which was used to represent biotic Fe(II) oxidation.³⁰ However, further investigation is required to understand the full range of redox chemistry which can be mediated by hematite.

Based on a combined understanding of Fe(II) driven recrystallization, and the biotic and abiotic redox cycling of Fe oxides, we investigate whether a DMRB or other electron source would be able to affect reduction of an electron acceptor, such as Cr, via hematite reduction, even when that source cannot directly react with this electron acceptor. Chromium is chosen as the terminal electron acceptor for these systems owing to its relevance for contaminated soils and sediments as well as serving as an ideal chemical probe for electron fate. This probe is needed to distinguish between reduction that occurs because of direct electron conduction versus indirect reduction by Fe(II) released from the hematite surface. Cr(VI) is a carcinogenic and highly soluble metal, and is often produced and released to soils and groundwater through industrial activities, while Cr(III) is relatively insoluble and has minimal toxicity.³¹⁻³³ Cr can be directly reduced by metal reducing microbes to form Cr(OH)₃, but can alternatively be reduced by Fe(II) to form mixed Fe/Cr hydroxide solids, which are typically in the form Cr_{1-x}Fe_x(OH)₃, where x is as large as 0.75.^{1,33-35} Indeed, Cr has already been used as a chemical probe to understand changes in Fe(II) activity during the redox cycling of goethite.³⁶ Thus, the type of Cr solid formed after reduction will be indicative of the source of the reducing electron (that is, Fe(II) or direct conduction). Numerous studies have shown redox coupling between bacteria and hematite or hematite and Cr, however, there appear to be no studies, if any, that demonstrate how these paired processes might operate simultaneously. The overarching goal of this work, therefore, was

to determine how hematite can link these two processes, resulting in a spatially segregated redox couple. This is accomplished through two experimental lines: 1) abiotic experiments, where a potentiostat provides current to a hematite sample immersed in a solution with Cr, and 2) biotic experiments, where the metal reducing bacteria *Shewanella Putrefaciens* is electrically connected to a hematite electrode that is immersed in a solution containing Cr. The results of these experiments are then used to determine how hematite semi-conductivity influences the coupling of these two redox reactions. The results of this work show that hematite acts as a mediator for reduction, allowing for reaction to occur between Cr and the electron source despite spatial segregation.

2. Materials and Methods

2.1 Experimental Set-up

Two electrochemical experimental systems were used to examine how hematite mediates the coupling between Cr reduction and bacterial metabolism: a potentiostatic setup where a DStat potentiostat provided the current for reduction, and a biotic setup where *S. Putrefaciens* provided the current for reduction (figure 1). The potentiostat was built following the given³⁷ instructions. Both experiments used a 3D printed two chamber system, a polished specular hematite electrode (Ward's Scientific, sample from Republic, MI), graphite electrode, and a coated paper cation exchange membrane (Membranes International, Inc.) which was used to separate the electrodes while allowing for charge equilibration. This experimental set up was chosen because it allowed for physical separation of bacteria and Cr, thus hematite would serve as the mediator for all redox reactions that occur. The potentiostatic experiments used a Ag/AgCl reference electrode to correctly set voltages. All electrodes were fabricated in house except for

one type of hematite electrode: a thin section of specular hematite mounted on silver epoxy which was prepared by Spectrum Petrographics™. Measurements of hematite resistivity were also taken to quantify the intrinsic variability of the hematite used to make electrodes (SI). Further details on the fabrication and handling of the electrodes and the chamber are included in the supplemental information.

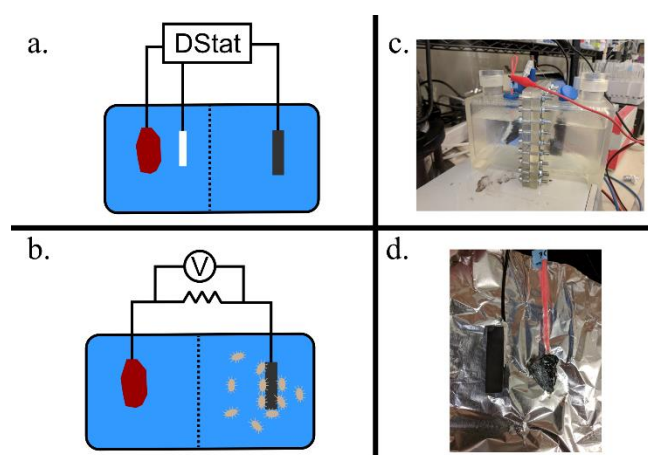


Figure 1: Experimental setups and materials. All experimental chambers are filled with a basal salt solution, and the chamber divided in half by a cation exchange membrane which prevented migration of Cr and bacteria. a. Schematic of potentiostatic experiments. The hematite electrode on the left chamber half is the working electrode for the DStat potentiostat, referenced to the Ag/AgCl reference electrode, while the carbon electrode is the counter electrode housed on the right chamber half. b. Schematic of biotic and control experiments. The left chamber half has a hematite electrode which is electrically connected to the carbon electrode on the right chamber half via a resistor. Current is generated by *S. Putrefaciens* which exists solely on the right half of the chamber, and potential drops are measured across the connecting resistor to determine

current. c. Photograph of a potentiostatic setup in an anoxic glove bag. d. Photograph of a carbon (left) and bulk hematite (right) electrode used in this work.

All experimental solutions used in these experiments were made in 18M Ω water with ACS grade chemicals. To ensure that *S. Putrefaciens* would perform metal reduction (as opposed to respiring oxygen) and to prevent premature oxidation of Fe or Cr, all experiments were performed in an anoxic glove bag (CoyLabs, 2-3% H₂, balance N₂). Solutions were prepared in normal laboratory air, purged with N₂ for at least 1 hour, and then immediately transferred to the anoxic glove bag. Measured oxygen levels in the glove bag were always below 1 ppm throughout experiments. A background basal salts solution (BSS) with a 50 mM sodium PIPES buffer concentration was used to fill the chambers for all experiments.³ A buffer was included in the BSS because hematite dissolution is known to increase solution pH. Initial experimental pHs were 7.1 ± 0.2 , and the only significant pH increase (0.8 pH units) was observed in an experiment where no Cr was included, likely due to hematite dissolution (Table 1, expt. A). Cr was added to experiments through a small volume spike of 50 mM potassium chromate stock to the chamber containing the hematite electrode, and there was no evidence of Cr migration across the cation exchange membrane in any experiment.

The primary differences between the two experiments was that of electrical configuration (figure 1). For potentiostatic experiments, the Dstat potentiostat was connected to the hematite, graphite, and reference electrode. It was controlled using a Python script to poise the hematite working electrode at -1000 mV vs. Ag/AgCl.^{37,38} In these experiments, the graphite electrode served as a counter electrode. Both the thin section hematite electrode and “bulk” hematite electrodes were used in these experiments as working electrodes. When using a thin section electrode, care was taken to ensure that the only conductive surface in contact with the

experimental solution was hematite. In potentiostatic experiments, currents provided to the working electrode were directly reported by the potentiostat using a built in measurement circuit.³⁷ For biotic experiments, the graphite and hematite electrodes were simply connected with a 100 Ω resistor, which provided sufficient resistance to allow for current measurement while not overly restricting current flow from *S. Putrefaciens*. For biotic experiments, a Keithley 2100 multimeter controlled by a Python script was used to measure and log voltages measured across the connected resistor, which was then converted to current.³⁸ Total amounts of electron transfer were calculated by integrating measured current in time using a trapezoidal method, as implemented in the NumPy package.³⁹

Sampling of experimental systems involved collection of aqueous samples, and in the potentiostatic experiment with a thin electrode, collection of the electrode itself. Aqueous samples collected from biotic experiments were filtered on 0.22 μm PES syringe filters to remove any possible bacteria. All samples were acidified within 12 hours after collection by the addition of 3 drops of 6N HCl, and were stored in plastic falcon tubes. Cr concentrations were measured in these samples using a Perkin Elmer NexIon 300-D ICP-MS and Fe in these samples through the Ferrozine method, which were then converted to mole amounts by using the solution volume calculated by changes in experimental mass.^{40,41} Further analytical details are available in the supplementary information.

2.2 Culture conditions

S. Putrefaciens, strain CN-32 (ATCC), was grown up from 50% glycerol stocks frozen at -80°C , in tryptic soy broth over a 16 hour period and harvested in the exponential growth phase by centrifugation and rinsing with BSS 3 times. On the final rinse, anoxic BSS was used. All

solutions used in biotic experiments were autoclaved at 121 °C prior to use, and all experimental surfaces (electrodes, chamber interiors, cation exchange membrane, etc.) were sterilized by either rinsing with 70% ethanol and drying in a biosafety cabinet, or by exposure to UV light for a minimum of 60 seconds. Bacteria were provided 10 mM lactate as a carbon source, and initial cell concentrations in experiments were 10^7 - 10^8 cells/mL, measured using the optical density at 660 nm as calibrated to measurements with a Guava flow cytometer.

Table 1 - Summary of experimental configurations. Uncertainties are the largest of either the ICP-MS measurement error (i.e. derived from the standard error of the calibration curve regression) or std. dev. of the replicate samples.

Experiment ID	Electron source	Hematite electrode type	Initial Cr Concentration (μ M)
A	DStat	Bulk	N.D.
B	DStat	Bulk	14.3 \pm 0.8
C	DStat	Thin	11.8 \pm 2.0
D	<i>S. Putrefaciens</i>	Bulk	22.5 \pm 1.1

2.3. XPS and Electron Microprobe Analysis

Finally, changes in the hematite surface were studied by comparing a polished thin electrode that was used in an experiment to one which had been left unreacted. The analyses could suggest potential reactions and solids that are forming at the electrode surface and evaluate the mechanism of Cr reduction. Once the electrode had been used in an experiment, it was dried and kept in an anoxic environment until just before analysis. An EOL-JXA-8200 Superprobe electron microprobe was used to collect electron backscatter images and Energy Dispersive X-

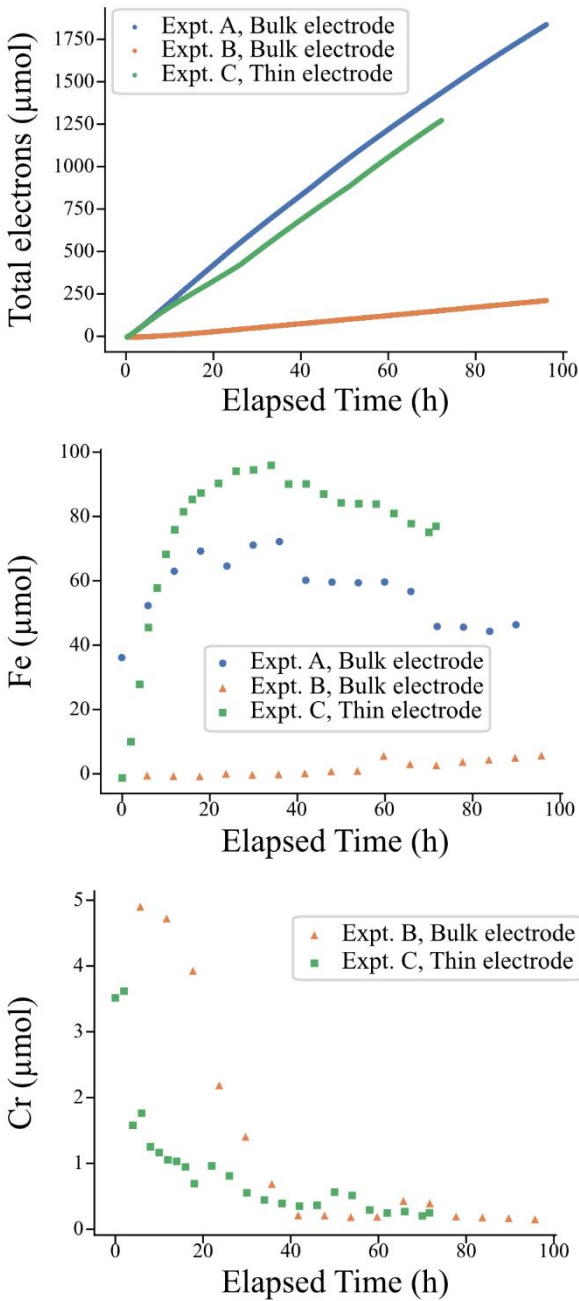


Figure 2: Graphs showing trends of electron transfer, dissolved Cr concentration, and dissolved Fe in potentiostatic experiments. In all experiments, the hematite electrode is poised to -1000mV vs. Ag/AgCl .

ray Spectroscopy (EDS) spectra of the thin electrode surfaces. The electron beam current was 2.5nA , and no additional electrode treatment was necessary to collect images. X-ray photoelectron spectroscopy (XPS) was performed on the unreacted and reacted thin electrodes using a Physical Electronics Versaprobe II x-ray photoelectron spectrometer to determine shifts in the relative molar abundance of different elements. Elemental peaks were fitted using Multipak software provided with the spectrometer.

3. Results and discussion

All experimental configurations are described in table 1. Control experiments without reduction (i.e. without a potentiostat) showed that the impact of sorption on Cr removal was minimal and that electron transfer would not occur without the inclusion of the potentiostat or the metal reducing bacteria

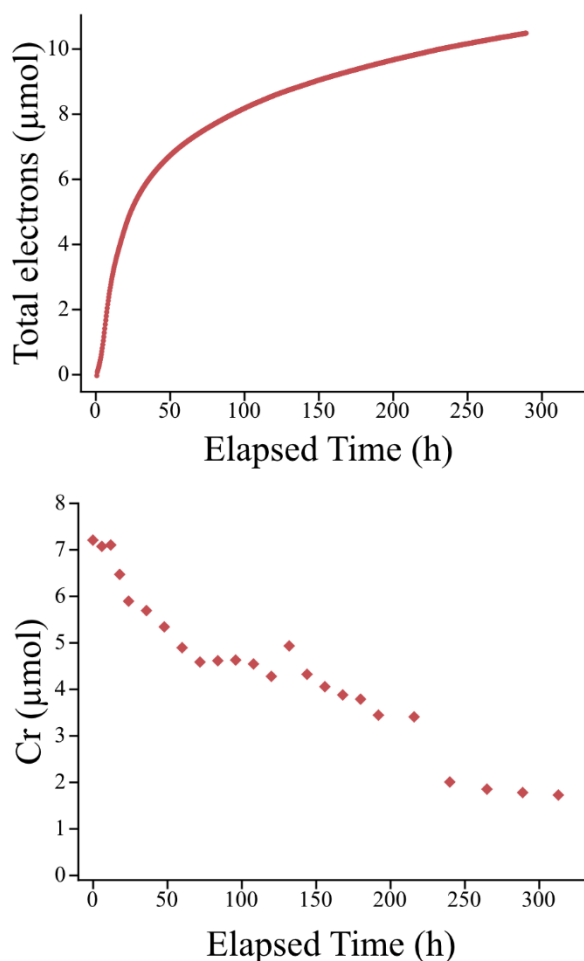


Figure 3: Results for current transfer and Cr changes in the hematite chamber from experiment D with *S. Putrefaciens* as the current generator.

(SI for details). Hematite resistivity was also calculated in three different samples of hematite varied significantly between the three samples, ranging from 500Ωm to nearly 11000Ωm, illustrating a significant heterogeneity in the hematite electrical properties, despite being from the same source material (See SI for details).

3.1 Dissolved Cr and Fe Time

series of measured Fe, Cr, and electron transfer during potentiostatic experiments (A, B and C from table 1) are shown in figure 2. Expt A, which used no Cr, and Expt. C, which used Cr and a thin section hematite electrode, had an order of magnitude larger Fe(II) released into solution (46 and 77 μmol Fe,

respectively) when compared to the experiment B (12 μmol), as well as significantly larger transferred electrons (A: 1842, B: 215, C: 1277 μmol electrons). Measurable Fe(III) was only observed in experiment A (figure S4). Fe(II) was also observed in the chamber containing the carbon electrode in this experiment to similar concentrations, indicating that Fe had crossed the

cation exchange membrane (figure S4). In potentiostatic experiments with Cr, dissolved amounts of Cr decreased by 96% (exp B) and 89% (exp C) in 40 hr. After ~40 hr, the dissolved Cr amount remained below detection levels. No Cr was detected in the carbon electrode chamber at any time point during the experiment. In experiment B, near complete Cr removal is observed prior to any appearance of Fe(II), while in experiment C, Cr removal and Fe(II) release occur simultaneously.

The results of the biotic experiment (D) are shown in figure 3. No form of Fe was detected in this experiment. In contrast with potentiostatic experiments, not all Cr was removed. The rate of Cr removal in this experiment was also slower than that observed in potentiostatic experiments B and C.

In both the biotic experiments and abiotic experiments, Cr was removed from solution, though at differing rates. Since the control experiments clearly demonstrated that sorption was not affecting the Cr concentrations, the only driver for this observed behavior is reduction, which must be associated with the current delivered. This is corroborated by the emergence of Fe(II) in potentiostatic experiments, which is a natural result of hematite reduction by the delivered current. Results from the dissolved concentrations of Cr do not, however, illustrate whether this reduction is the result of electrons directly being conducted to Cr associated with the hematite surface, or if this is the result of indirect reduction by Fe(II) released from the hematite surface.

Dissolved Fe(II) was only observed in potentiostatic experiments (A, B, C), but the amounts of dissolved Fe(II) varied (Figure 2). These variations, including the lack of observed dissolved Fe(II) in experiment D, track well with the variations in the total electrons transferred between these experiments. Delivered electrons result in reduction of hematite, thus Fe(II) production is mechanistically linked to the amount of current transfer. The number of electrons

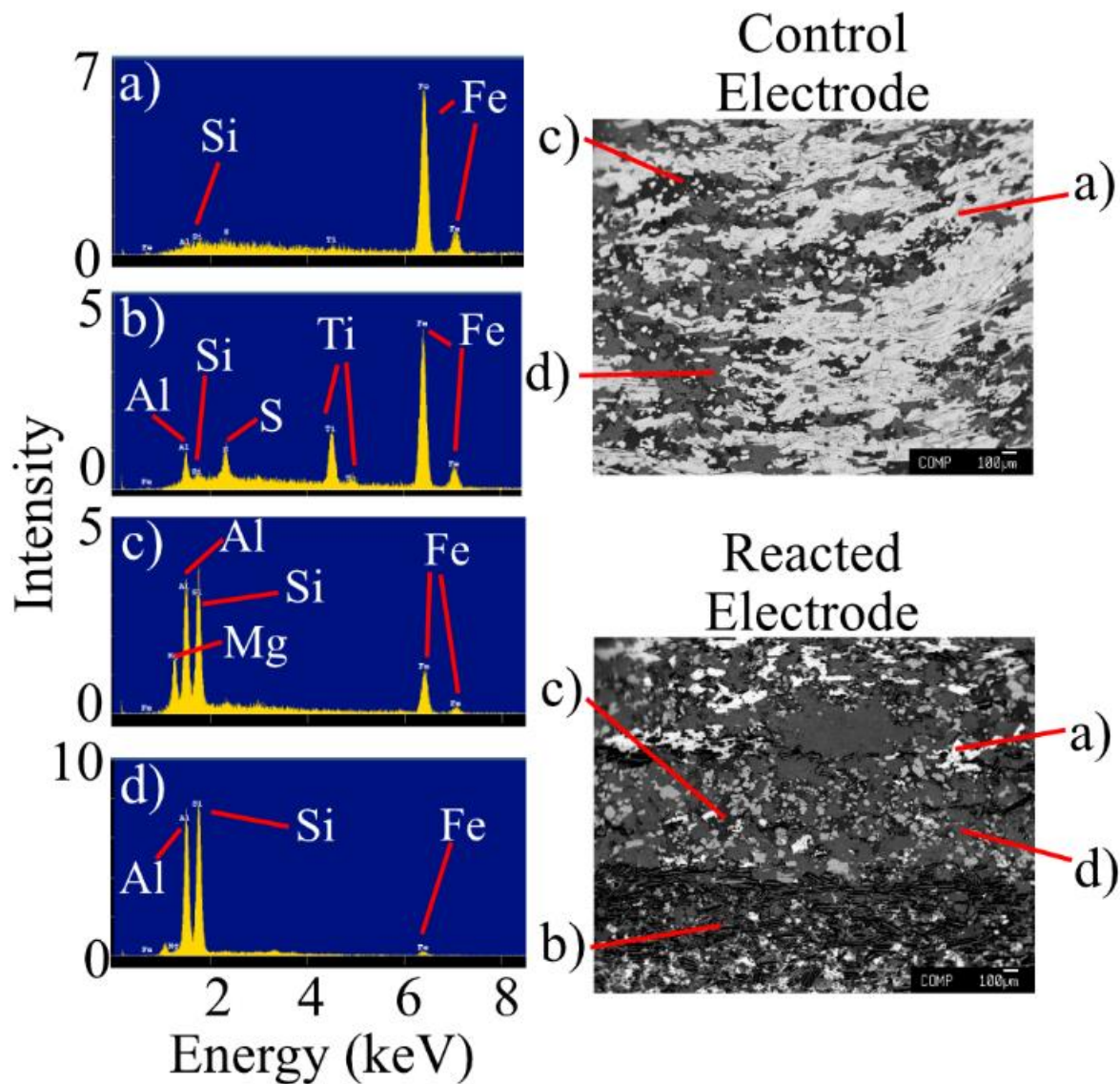


Figure 4: EDS spectra (left) and electron backscatter images (right) of polished thin hematite electrodes collected via an electron microprobe. The spectra of labeled components a,c and d did not differ between the control (unreacted) electrode and reacted electrode, while component b was only observed in the reacted electrode.

transferred varied widely between experiments even under similar conditions, which is most likely due to the intrinsic variations in resistivity of the hematite used in this study. These variations are discussed in depth in the supporting information.

Surface chemistry results

To better understand the fate of reduced Cr and Fe, Electron backscatter images, EDS spectra, and XPS spectra were collected to characterize changes in surface of the thin electrode used in a potentiostatic experiment (figure 4 for backscatter images and EDS, S5 for XPS spectra). As shown in Figure 4, an unreacted hematite electrode has a widespread Fe phase (in white, labeled a) that is most likely the hematite, as well as two other phases (c,d) corresponding to Al-Si minerals. In the reacted electrode, the widespread Fe phase seen in unreacted hematite electrode has been replaced with an alternate Fe phase (labeled b in Figure 4) that shows differences in the EDS spectra from the original Fe phase. The variability of the hematite surface observed further supports the assertion that the hematite used here had significant intrinsic variability which lead to variations in its resistivity (SI). No Cr was detected on the reacted electrode surface using the electron microprobe, however, the Cr amounts used were likely too low to detect using an electron microprobe. XPS spectra were collected to determine relative ratios of elemental species at the electrode surface, and had sufficient sensitivity to detect Cr (SI FOR SPECTRA). Cr was not detected at any point in the unreacted electrode, while Cr/Fe ratios ranged from 0.00 (i.e. no Cr) to 0.53 in the reacted thin electrode. Additional information from both analyses (raw spectra, other analyzed elements, additional images, etc.) are given in the supplementary information.

The Cr peak observed in the XPS spectra of the reacted hematite electrode indicates that the Cr is associated with the hematite surface (Figure S5). Moreover, heterogeneity in surface Cr distribution was also observed in the XPS measurements, as evidenced by the different Cr/Fe ratios observed. Previous studies of Cr reduction in the presence of Fe showed that Cr will form a mixed Cr/Fe solid when exposed to Fe(II), with Cr/Fe ratios as low as 0.33, as opposed to forming a pure phase Cr(OH)₃ when directly reduced.³⁴⁻³⁶ Multiple locations on the hematite

surface (5 of 21) have Fe/Cr ratios within the range of a mixed Cr/Fe solid (SI Tables S1 and S2). The largest Cr/Fe ratio observed in the XPS results is 0.5, which would still correspond to a mixed Cr/Fe solid, rather than a pure Cr phase. While these results positively identify the formation of the mixed Cr/Fe solid as a major pathway for Cr reduction, they do not necessarily eliminate the possibility of some direct reduction, which would form Cr hydroxide solids. However, the surface analyses here strongly suggest that indirect reduction by Fe(II) is a major source of Cr reduction in these experiments.

The indirect reduction process also explains why the timing of Fe(II) release and Cr reduction vary between experiments (i.e. that in expt. B Cr reduction precedes Fe(II) release, while in expt. C, they occur simultaneously). If the delivered current produces Fe(II) at a rate faster than Cr reduction by Fe(II) can occur, then both Cr removal and Fe(II) release would occur simultaneously. This hypothesis is further supported by the variations in electron transfer, where experiment C had more electrons transferred (and therefore a higher current) compared to experiment B. Lastly, this would then explain why no dissolved Fe(II) is observed in the biotic experiment D, as the current, and therefore, Fe(II) reduction rate, were much lower than the rate of Cr reduction by Fe(II).

Electron and Mass Balance

To finalize a conceptual model of the mechanisms at play, it is valuable to compare the total transferred electrons to the amount of observed Cr and Fe reduction to complete the electron and mass balance. Since reduction is the only source of Cr removal, it is relatively simple to do this for Cr by considering the relevant half reaction:



Therefore, the total mol of Cr removed is 3x the electrons required to drive this reduction. Table 2 summarizes the amount of calculated Cr reduction in each experiment with Cr (B, C, D), based on the total electrons delivered during Cr reduction. In potentiostatic experiments B and C, while all of the Cr is removed from solution, there are significantly more electrons measured via the current compared to that required to create the observed Cr reduction. The remaining electrons most likely result in Fe reduction, which will be discussed below.

Experiment ID	Cr reduced (μmol)	e^- transfer implied by Cr reduction (μmol)	Measured e^- transfer (μmol)
B	4.7	14.1	79.4
C	3.1	9.3	583
D	5.5	16.5	10.5

Table 2 - Comparison of Cr loss by reduction to electron transfer. Electrons transferred are windowed to the period in which Cr loss is observed. In the case of potentiostatic experiments, this is partway through the experiment, while in biotic experiments, the entire experimental time is considered.

The case of the biotic experiment presents an opposite trend however: the amount of electrons implied by Cr reduction is larger than the measured current. Based on the collected data, the reasons for such anomalous high Cr reduction in biotic experiment remain unexplained. This type of

discrepancy was previously observed in studies of Cr reduction by Fe(II) in the presence of organic matter.⁴² In that work, Cr “autoreduction” by organic ligands present in the natural mineral drove the excess Cr. In that case, Fe(II) only contributed to the rate limiting step of Cr(VI) reduction to Cr(V) and subsequent reduction of Cr(V) all the way to Cr(III) was performed by photochemically produced oxygen radicals from the organic matter.^{1,43} Although, there’s no organic matter available to provide those radicals in these experiments, hematite is a well-known photocatalyst that may serve a similar role in this system, where light stimulates photochemistry that reduces Fe or Cr.^{14,30,44} The hematite films used for those purposes, however

is of much higher purity from that of the natural mineral here, nor was there specific control for the lighting conditions in these experiments, which make it difficult to determine if light would have such a measurable impact. While beyond of the scope of the work performed here, additional work that quantifies the potential for photocatalyzed reduction by natural hematite samples would be invaluable both for a better understanding of Cr dynamics as well as how the photocatalytic properties of natural hematite samples may influence aquatic geochemistry.

A similar process can be applied to Fe to complete the balance of electron transfer, in which each mol of Fe(II) measured accounts for a mol of the transferred electrons, following the half reaction:



For the biotic experiment D, no dissolved Fe is measured and the electron balance is already complete (barring the excess reduction observed). However, as evident in Figure 2, the dissolved Fe measured in potentiostatic experiments is an order of magnitude smaller than the total electrons transferred, even considering Fe that has crossed the cation exchange membrane to the carbon electrode side is considered (Figure S4). The only other potential redox reaction in this system would be splitting of water into hydrogen and oxygen, however, no gas evolution was observed in any experiment. Any measured current beyond that which contributes to Cr reduction must, therefore, result in Fe reduction. The electron backscatter images and EDS spectra support this assertion, as evidenced by the significant change in surface morphology after use in the experiment. The electrode surface, which was originally populated with a “bright” Fe solid have transformed into a darker Fe solid with a different EDS spectra. The physical and compositional transformations are clearly indicative of reductive Fe dissolution by the delivered current, however this does not constrain the fate of Fe(II) that is not observed in solution.

The fate of Fe(II) cannot be completely determined directly from the analyses performed here, but there are a few reasonable possibilities: (1) Fe(II) generated remains sorbed to the hematite electrode surface. Indeed, Fe(II) sorption to Fe (oxy)hydroxides is well documented and has previously been observed during cyclic oxidation and reduction of goethite.²¹ In those experiments, reduced Fe(II) persisted even throughout oxic conditions by associating with the surface, so it is very likely at least some amount of Fe(II) would be retained on the surface.^{36,45} The dissolved Fe(II) forms a precipitate on the hematite surface, which is what comprises the “new” phase observed in electron backscatter images after use in the experimental set up, which has been observed in other studies of hematite redox cycling.^{9,46,47} Both sorption of reduced Fe as

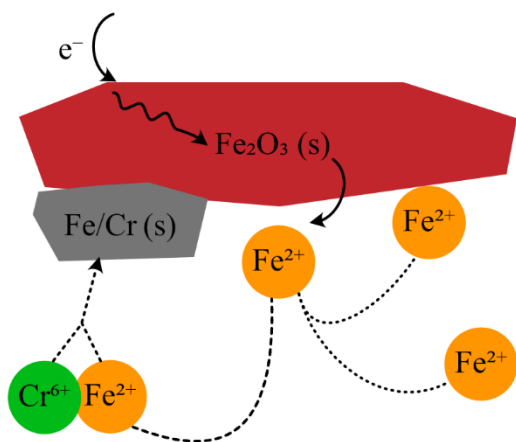


Figure 2-Schematic of conceptual model which illustrates how electrons interact with hematite to reduce Fe and Cr. Conducted electrons from an arbitrary source produce Fe(II) which can either reduce Cr to form a solid or remain as Fe(II) to distribute between sorbed and dissolved species.

well as precipitation of other Fe minerals is reasonable here and would readily close the balance of electrons, however, further studies are needed that explicitly track Fe fate, such as through the use of an isotopically labeled Fe tracer. Overall, the closure of the Cr, Fe, and electron balances illustrates a picture of the dynamics at play in these experiments.

Proposed Mechanism

Figure 5 proposes a conceptual model for this experimental system based on the above analyses, illustrating the fate of Cr, Fe, and electrons in this experimental system. Electrons that arrive at the hematite

electrode, regardless of their origin, dissolve hematite, producing Fe(II) at the interface of the hematite electrode and solution. The resulting Fe(II) most likely reduces Cr to form mixed Fe/Cr solids, with perhaps some direct reduction occurring. When the rate of Cr reduction is slower than the delivered current or all Cr has been reductively precipitated, excess Fe(II) is produced. This Fe can be found both in solution and associated in some way with the hematite electrode. This proposed mechanism is a natural extension of the established mechanism behind Fe(II) catalyzed recrystallization; the main difference here from those works is that there is a separate source of electrons as well as a terminal electron acceptor instead of Fe(II) as electron source and terminal electron acceptor.^{22-24,30} These results demonstrate that hematite, or other semi-conductive Fe minerals, may serve a broader role in controlling redox chemistry in natural soils.

Implications for environmental processes

The results of this work have immediate and direct implications for the cycling and remediation of Cr in natural groundwaters, as they clearly demonstrate that semiconducting Fe oxide minerals are able to effectively distribute donated electrons beyond their source. Fe(0) is often used in permeable reactive barriers to remediate groundwaters contaminated with Cr(VI), however, their efficacy decreases in time due to the formation of passivating mixed Fe/Cr solids that prevent further reaction.^{34,48,49} It may be possible to include hematite into these reactive barriers in such a way that the reduction of Cr occurs at a separate location from Fe(0), which is the electron source, thereby extending the life and remediation capacity of these reactive barrier systems. Alternatively, it may eventually be possible to build hematite “antennas” into a Cr contaminated groundwater system which can be poised at a reducing potential and therefore drive Cr reduction. The results of this work lay the foundation for these developments, though

further investigation is required to better understand how to engineer this mechanism into a remediation strategy.

Dissimilatory metal reducing bacteria (DMRB) are well established to rely heavily on Fe hydr(oxides), such as hematite, as an electron acceptor during anaerobic metabolism, and the results here add potential interactions between an Fe oxide and DMRB. The biotic experimental results clearly demonstrated that hematite created a coupling between microbial metabolism of lactate and Cr reduction, implying that semiconductive phases, such as hematite, may enabling the coupling of other redox processes. One prominent example is direct interspecies electron transfer (DIET), where one bacterial species will donate the electrons from their metabolism to another species.^{50,51} The observed coupling of reactions here supports the possibility that bacterial communities could use hematite as a mediator for these electron transfers. These results are also in good alignment with assertions that bacteria can use conductive substrates (i.e. minerals, other bacteria) to form bacterially active networks, as metal reducing bacteria here used hematite to access Cr as a terminal electron acceptor.^{13,51-54} Further investigation is required to understand the prevalence of these networks in natural soils and their importance to bacterial growth in natural settings.

Some of the earliest electrochemical studies, where sacrificial anodes were used to prevent oxidation of metal ship components, established that electrical contact was sufficient to couple redox reactions of different metals that were otherwise separated.^{55,56} This work follows in the footsteps of that foundational work: hematite enabled spatially segregated redox coupling between a metal reducing bacteria or other electron source, and Cr. The results of this work, however, outline only the first steps of broader understanding of how mineral conductivity may influence groundwater chemistry. Fe(II) forms favorable redox couples with other priority

contaminants such as U or As, and this mechanism could play a role in the remediation or natural cycling of those contaminants.^{3,57–60} Fe(II) catalyzed recrystallization has been demonstrated for goethite, another semi-conducting Fe mineral, thus the results here also imply that this conduction mechanism may be more broadly applicable wherever Fe cycling occurs. Further investigation is needed, however, to demonstrate the range of biogeochemical systems where this mechanism is relevant, further understand the influence of these processes on hematite surface chemistry and illustrate the importance for this mechanism in natural soils and groundwater.

References

- (1) Buerge, I. J.; Hug, S. J. Kinetics and PH Dependence of Chromium(VI) Reduction by Iron(II). *Environmental Science & Technology* **1997**, *31* (5), 1426–1432. <https://doi.org/10/cs4k46>.
- (2) Stewart, S. M.; Hofstetter, T. B.; Joshi, P.; Gorski, C. A. Linking Thermodynamics to Pollutant Reduction Kinetics by Fe²⁺ Bound to Iron Oxides. *Environ. Sci. Technol.* **2018**, *52* (10), 5600–5609. <https://doi.org/10.1021/acs.est.8b00481>.
- (3) Kocar, B. D.; Herbel, M. J.; Tufano, K. J.; Fendorf, S. Contrasting Effects of Dissimilatory Iron (III) and Arsenic (V) Reduction on Arsenic Retention and Transport. *Environmental Science & Technology* **2006**, *40* (21), 6715–6721. <https://doi.org/10.1021/es061540k>.
- (4) Jeon, B.-H.; Dempsey, B. A.; Burgos, W. D.; Barnett, M. O.; Roden, E. E. Chemical Reduction of U(VI) by Fe(II) at the Solid–Water Interface Using Natural and Synthetic Fe(III) Oxides. *Environmental Science & Technology* **2005**, *39* (15), 5642–5649. <https://doi.org/10.1021/es0487527>.
- (5) Johnston, C. P.; Chrysochoou, M. Mechanisms of Chromate Adsorption on Hematite. *Geochimica et Cosmochimica Acta* **2014**, *138*, 146–157. <https://doi.org/10/f6bbj9>.
- (6) Bargar, J. R.; Reitmeyer, R.; Davis, J. A.; John R. Bargar, *, †; Rebecca Reitmeyer, ‡ and; Davis‡, J. A. Spectroscopic Confirmation of Uranium(VI)–Carbonato Adsorption Complexes on Hematite. *Environmental Science & Technology* **1999**, *33* (14), 2481–2484. <https://doi.org/10.1021/es990048g>.
- (7) Renock, D.; Mueller, M.; Yuan, K.; Ewing, R. C.; Becker, U. The Energetics and Kinetics of Uranyl Reduction on Pyrite, Hematite, and Magnetite Surfaces: A Powder Microelectrode Study. *Geochimica et Cosmochimica Acta* **2013**, *118*, 56–71. <https://doi.org/10.1016/j.gca.2013.04.019>.
- (8) Dong, Y.; Sanford, R. A.; Chang, Y.; McInerney, M. J.; Fouke, B. W. Hematite Reduction Buffers Acid Generation and Enhances Nutrient Uptake by a Fermentative Iron Reducing Bacterium, *Orenia Metallireducens* Strain Z6. *Environmental Science & Technology* **2017**, *51* (1), 232–242. <https://doi.org/10.1021/acs.est.6b04126>.
- (9) Behrends, T.; Van Cappellen, P. Transformation of Hematite into Magnetite During Dissimilatory Iron Reduction - Conditions and Mechanisms. *Geomicrobiology Journal* **2007**, *24* (5), 403–416. <https://doi.org/10/c652dm>.

- (10) Dixit, S.; Hering, J. G. Comparison of Arsenic(V) and Arsenic(III) Sorption onto Iron Oxide Minerals: Implications for Arsenic Mobility. *Environmental Science & Technology* **2003**, *37* (18), 4182–4189. <https://doi.org/10.1021/es030309t>.
- (11) Dzombak, D.A.; Morel, F.M.M. *Surface Complexation Modeling: Hydrous Ferric Oxide*; Wiley: New York, NY, 1990.
- (12) Alexandratos, V. G.; Behrends, T.; Van Cappellen, P. Fate of Adsorbed U(VI) during Sulfidization of Lepidocrocite and Hematite. *Environmental Science & Technology* **2017**, *51* (4), 2140–2150. <https://doi.org/10.1021/acs.est.6b05453>.
- (13) Meitl, L. A.; Eggleston, C. M.; Colberg, P. J. S.; Khare, N.; Reardon, C. L.; Shi, L. Electrochemical Interaction of *Shewanella Oneidensis* MR-1 and Its Outer Membrane Cytochromes OmcA and MtrC with Hematite Electrodes. *Geochimica et Cosmochimica Acta* **2009**, *73* (18), 5292–5307. <https://doi.org/10.1016/j.gca.2009.06.021>.
- (14) Eggleston, C. M. Toward New Uses for Hematite. *Science* **2008**, *320* (5873), 184–185. <https://doi.org/10/c63spq>.
- (15) Lovley, D. R. Dissimilatory Metal Reduction. *Annual review of microbiology* **1993**, *47* (II), 263–290. <https://doi.org/10.1146/annurev.micro.47.1.263>.
- (16) Michelson, K.; Sanford, R. A.; Valocchi, A. J.; Werth, C. J. Nanowires of *Geobacter Sulfurreducens* Require Redox Cofactors to Reduce Metals in Pore Spaces Too Small for Cell Passage. *Environmental Science & Technology* **2017**, *51* (20), 11660–11668. <https://doi.org/10.1021/acs.est.7b02531>.
- (17) Reguera, G.; McCarthy, K. D.; Mehta, T.; Nicoll, J. S.; Tuominen, M. T.; Lovley, D. R. Extracellular Electron Transfer via Microbial Nanowires. *Nature* **2005**, *435* (7045), 1098–1101. <https://doi.org/10.1038/nature03661>.
- (18) Gorby, Y. A.; Yanina, S.; McLean, J. S.; Rosso, K. M.; Moyles, D.; Dohnalkova, A.; Beveridge, T. J.; Chang, I. S.; Kim, B. H.; Kim, K. S.; Culley, D. E.; Reed, S. B.; Romine, M. F.; Saffarini, D. a; Hill, E. A.; Shi, L.; Elias, D. A.; Kennedy, D. W.; Pinchuk, G.; Watanabe, K.; Ishii, S.; Logan, B.; Nealson, K. H.; Fredrickson, J. K. Electrically Conductive Bacterial Nanowires Produced by *Shewanella Oneidensis* Strain MR-1 and Other Microorganisms. *Proceedings of the National Academy of Sciences of the United States of America* **2006**, *103* (30), 11358–11363. <https://doi.org/10.1073/pnas.0604517103>.
- (19) Logan, B. E.; Hamelers, B.; Rozendal, R.; Schröder, U.; Keller, J.; Freguia, S.; Aelterman, P.; Verstraete, W.; Rabaey, K. Microbial Fuel Cells: Methodology and Technology. *Environmental Science and Technology* **2006**, *40* (17), 5181–5192. <https://doi.org/10.1021/es0605016>.
- (20) Min, B.; Cheng, S.; Logan, B. E. Electricity Generation Using Membrane and Salt Bridge Microbial Fuel Cells. *Water Research* **2005**, *39* (9), 1675–1686. <https://doi.org/10.1016/j.watres.2005.02.002>.
- (21) Gorski, C. A.; Scherer, M. M. Fe²⁺ Sorption at the Fe Oxide-Water Interface: A Revised Conceptual Framework. *ACS Symposium Series* **2011**, *1071*, 315–343. <https://doi.org/10.1021/bk-2011-1071.ch015>.
- (22) Handler, R. M.; Frierdich, A. J.; Johnson, C. M.; Rosso, K. M.; Beard, B. L.; Wang, C.; Latta, D. E.; Neumann, A.; Pasakarnis, T.; Premaratne, W. A. P. J.; Scherer, M. M. Fe(II)-Catalyzed Recrystallization of Goethite Revisited. *Environmental Science and Technology* **2014**, *48* (19), 11302–11311. <https://doi.org/10.1021/es503084u>.
- (23) Yanina, S. V.; Rosso, K. M. Linked Reactivity at Mineral-Water Interfaces Through Bulk Crystal Conduction. *Science* **2008**, *320* (5873), 218–222. <https://doi.org/10/cdxbt9>.

- (24) Frierdich, A. J.; Helgeson, M.; Liu, C.; Wang, C.; Rosso, K. M.; Scherer, M. M. Iron Atom Exchange between Hematite and Aqueous Fe(II). *Environmental Science and Technology* **2015**, *49* (14), 8479–8486. <https://doi.org/10.1021/acs.est.5b01276>.
- (25) Gorski, C. A.; Fantle, M. S. Stable Mineral Recrystallization in Low Temperature Aqueous Systems: A Critical Review. *Geochimica et Cosmochimica Acta* **2017**, *198*, 439–465. <https://doi.org/10.1016/j.gca.2016.11.013>.
- (26) Zarzycki, P.; Rosso, K. M. Stochastic Simulation of Isotopic Exchange Mechanisms for Fe(II)-Catalyzed Recrystallization of Goethite. *Environmental Science and Technology* **2017**, *51* (13), 7552–7559. <https://doi.org/10.1021/acs.est.7b01491>.
- (27) Nico, P. S.; Stewart, B. D.; Fendorf, S. Incorporation of Oxidized Uranium into Fe (Hydr)Oxides during Fe(II) Catalyzed Remineralization. *Environmental Science and Technology* **2009**, *43* (19), 7391–7396. <https://doi.org/10.1021/es900515q>.
- (28) Latta, D. E.; Gorski, C. A.; Scherer, M. M. Influence of Fe²⁺-Catalysed Iron Oxide Recrystallization on Metal Cycling. *Biochemical Society Transactions* **2012**, *40* (6), 1191–1197. <https://doi.org/10/f4d2rm>.
- (29) Xiao, W.; Jones, A. M.; Li, X.; Collins, R. N.; Waite, T. D. Effect of *Shewanella Oneidensis* on the Kinetics of Fe(II)-Catalyzed Transformation of Ferrihydrite to Crystalline Iron Oxides. *Environmental Science & Technology* **2017**, No. ii, acs.est.7b05098-ac. est.7b05098. <https://doi.org/10.1021/acs.est.7b05098>.
- (30) Liu, T.; Wang, Y.; Liu, C.; Li, X.; Cheng, K.; Wu, Y.; Fang, L.; Li, F.; Liu, C. Conduction Band of Hematite Can Mediate Cytochrome Reduction by Fe(II) under Dark and Anoxic Conditions. *Environmental Science & Technology* **2020**, *54* (8), 4810–4819. <https://doi.org/10/ghfkh7>.
- (31) Hausladen, D. M.; Alexander-Ozinskas, A.; McClain, C.; Fendorf, S. Hexavalent Chromium Sources and Distribution in California Groundwater. *Environmental Science & Technology* **2018**, *52* (15), 8242–8251. <https://doi.org/10/gd4ksz>.
- (32) Hausladen, D. M.; Fendorf, S. Hexavalent Chromium Generation within Naturally Structured Soils and Sediments. *Environmental Science & Technology* **2017**, *51* (4), 2058–2067. <https://doi.org/10/f9pznv>.
- (33) Richard, F. C.; Bourg, A. C. M. Aqueous Geochemistry of Chromium: A Review. *Water Research* **1991**, *25* (7), 807–816. <https://doi.org/10/dw3tth>.
- (34) Hansel, C. M.; Wielinga, B. W.; Fendorf, S. Structural and Compositional Evolution of Cr/Fe Solids after Indirect Chromate Reduction by Dissimilatory Iron-Reducing Bacteria. *Geochimica et Cosmochimica Acta* **2003**, *67* (3), 401–412. [https://doi.org/10.1016/S0016-7037\(02\)01081-5](https://doi.org/10.1016/S0016-7037(02)01081-5).
- (35) Fendorf, S.; Wielinga, B. W.; Hansel, C. M. Chromium Transformations in Natural Environments: The Role of Biological and Abiological Processes in Chromium(VI) Reduction. *International Geology Review* **2000**, *42* (8), 691–701. <https://doi.org/10.1080/00206810009465107>.
- (36) Tomaszewski, E. J.; Lee, S.; Rudolph, J.; Xu, H.; Ginder-Vogel, M. The Reactivity of Fe(II) Associated with Goethite Formed during Short Redox Cycles toward Cr(VI) Reduction under Oxidic Conditions. *Chemical Geology* **2017**, *464*, 101–109. <https://doi.org/10.1016/j.chemgeo.2017.01.029>.
- (37) Dryden, M. D. M.; Wheeler, A. R. DStat: A Versatile, Open-Source Potentiostat for Electroanalysis and Integration. *PLoS ONE* **2015**, *10* (10), 1–17. <https://doi.org/10.1371/journal.pone.0140349>.

- (38) Python Software Foundation. Python Language Reference <https://www.python.org/>. <https://doi.org/10.1201/9781584889304.axd>.
- (39) Jones, E.; Oliphant, E.; Peterson, P. SciPy: Open source scientific tools for Python www.scipy.org.
- (40) Stookey, L. L. Ferrozine---a New Spectrophotometric Reagent for Iron. *Analytical Chemistry* **1970**, *42* (7), 779–781. <https://doi.org/10.1021/ac60289a016>.
- (41) Viollier, E.; Inglett, P. W.; Hunter, K.; Roychoudhury, A. N.; Van Cappellen, P. The Ferrozine Method Revisited: Fe(II)/Fe(III) Determination in Natural Waters. *Applied Geochemistry* **2000**, *15* (6), 785–790. [https://doi.org/10.1016/S0883-2927\(99\)00097-9](https://doi.org/10.1016/S0883-2927(99)00097-9).
- (42) Whitaker, A. H.; Peña, J.; Amor, M.; Duckworth, O. W. Cr(VI) Uptake and Reduction by Biogenic Iron (Oxyhydr)Oxides. *Environ. Sci.: Processes Impacts* **2018**, *20* (7), 1056–1068. <https://doi.org/10/gfx5c3>.
- (43) Schwarzenbach, R. P.; Angst, W.; Holliger, C.; Hug, J.; Klausen, J. Reductive Transformations of Anthropogenic Chemicals in Natural and Technical Systems. *Chimia* **1997**, *51*, 908–914.
- (44) Tamirat, A. G.; Rick, J.; Dubale, A. A.; Su, W.-N.; Hwang, B.-J. Using Hematite for Photoelectrochemical Water Splitting: A Review of Current Progress and Challenges. *Nanoscale Horiz.* **2016**, *1* (4), 243–267. <https://doi.org/10/ggxxgzd>.
- (45) Tomaszewski, E. J.; Cronk, S. S.; Gorski, C. A.; Ginder-Vogel, M. The Role of Dissolved Fe(II) Concentration in the Mineralogical Evolution of Fe (Hydr)Oxides during Redox Cycling. *Chemical Geology* **2016**, *438*, 163–170. <https://doi.org/10/f83f24>.
- (46) Liu, C.; Zachara, J. M.; Gorby, Y. A.; Szecsody, J. E.; Brown, C. F. Microbial Reduction of Fe(III) and Sorption/Precipitation of Fe(II) on *Shewanella Putrefaciens* Strain CN32. *Environmental Science and Technology* **2001**, *35* (7), 1385–1393. <https://doi.org/10.1021/es0015139>.
- (47) Boland, D. D.; Collins, R. N.; Glover, C. J.; David Waite, T. An in Situ Quick-EXAFS and Redox Potential Study of the Fe(II)-Catalysed Transformation of Ferrihydrite. *Colloids and Surfaces A: Physicochemical and Engineering Aspects* **2013**, *435*, 2–8. <https://doi.org/10.1016/j.colsurfa.2013.02.009>.
- (48) Gheju, M.; Balcu, I. Removal of Chromium from Cr(VI) Polluted Wastewaters by Reduction with Scrap Iron and Subsequent Precipitation of Resulted Cations. *Journal of Hazardous Materials* **2011**, *196*, 131–138. <https://doi.org/10/cn3c27>.
- (49) Deng, Y.; Stjernström, M.; Banwart, S. Accumulation and Remobilization of Aqueous Chromium(VI) at Iron Oxide Surfaces: Application of a Thin-Film Continuous Flow-through Reactor. *Journal of Contaminant Hydrology* **1996**, *21* (1), 141–151. <https://doi.org/10/ck2jh6>.
- (50) Rotaru, A. E.; Shrestha, P. M.; Liu, F.; Markovaite, B.; Chen, S.; Nevin, K. P.; Lovley, D. R. Direct Interspecies Electron Transfer between *Geobacter Metallireducens* and *Methanosarcina Barkeri*. *Applied and Environmental Microbiology* **2014**, *80* (15), 4599–4605. <https://doi.org/10.1128/AEM.00895-14>.
- (51) Lovley, D. R. Happy Together: Microbial Communities That Hook up to Swap Electrons. *The ISME Journal* **2016**, *11* (2), 1–10. <https://doi.org/10.1038/ismej.2016.136>.
- (52) Nakamura, R.; Kai, F.; Okamoto, A.; Newton, G. J.; Hashimoto, K. Self-Constructed Electrically Conductive Bacterial Networks. *Angewandte Chemie International Edition* **2009**, *48* (3), 508–511. <https://doi.org/10/bh2c5n>.

- (53) Kato, S.; Nakamura, R.; Kai, F.; Watanabe, K.; Hashimoto, K. Respiratory Interactions of Soil Bacteria with (Semi)Conductive Iron-Oxide Minerals. *Environmental Microbiology* **2010**, *12* (12), 3114–3123. <https://doi.org/10/bs5w2m>.
- (54) Nielsen, L. P.; Risgaard-Petersen, N.; Fossing, H.; Christensen, P. B.; Sayama, M. Electric Currents Couple Spatially Separated Biogeochemical Processes in Marine Sediment. *Nature* **2010**, *463* (7284), 1071–1074. <https://doi.org/10/fsdphg>.
- (55) Davy, H. XII. Additional Experiments and Observations on the Application of Electrical Combinations to the Preservation of the Copper Sheathing of Ships, and to Other Purposes. *Philosophical Transactions of the Royal Society of London* **1824**, *114*, 242–246. <https://doi.org/10/bm3czz>.
- (56) Davy, H. VI. On the Corrosion of Copper Sheeting by Sea Water, and on Methods of Preventing This Effect; and on Their Application to Ships of War and Other Ships. *Philosophical Transactions of the Royal Society of London* **1824**, *114*, 151–158. <https://doi.org/10/dt6bq8>.
- (57) Pearce, C. I.; Wilkins, M. J.; Zhang, C.; Heald, S. M.; Fredrickson, J. K.; Zachara, J. M. Pore-Scale Characterization of Biogeochemical Controls on Iron and Uranium Speciation under Flow Conditions. *Environmental Science and Technology* **2012**, *46* (15), 7992–8000. <https://doi.org/10.1021/es301050h>.
- (58) Liger, E.; Charlet, L.; Cappellen, P. V. Surface Catalysis of Uranium (VI) Reduction by Iron (II). *Geochimica et Cosmochimica Acta* **1999**, *63* (19), 2939–2955. [https://doi.org/10.1016/S0016-7037\(99\)00265-3](https://doi.org/10.1016/S0016-7037(99)00265-3).
- (59) Amstaetter, K.; Borch, T.; Larese-Casanova, P.; Kappler, A. Redox Transformation of Arsenic by Fe(II)-Activated Goethite (α -FeOOH). *Environmental Science & Technology* **2010**, *44* (1), 102–108. <https://doi.org/10.1021/es901274s>.
- (60) Newsome, L.; Lopez Adams, R.; Downie, H. F.; Moore, K. L.; Lloyd, J. R. NanoSIMS Imaging of Extracellular Electron Transport Processes during Microbial Iron(III) Reduction. *FEMS Microbiol Ecol* **2018**, *94* (8). <https://doi.org/10/gdt2rb>.

Acknowledgements

The authors would like to thank Dr. Nilanjan Chatterjee (MIT) for his assistance in operating the electron microprobe, Libby Shaw (MIT) for her assistance in collecting the XPS spectra for the samples, Allison Coe (MIT) for her assistance in quantifying *S. Putrafaciens* concentrations, and Professors Charles Harvey (MIT) and Harold Hemond (MIT) for their advice on the characterization of the hematite and general feedback on this work. This work was partially supported by the MIT Department of Civil and Environmental Engineering. The authors declare no competing financial interest.

for details.